PHYSICAL REVIEW B
CONDENSED MATTER

THIRD SERIES, VOLUME 34, NUMBER 8 PART I 15 OCTOBER 1986

Tunneling microscopy study of the graphite surface in air and water

J. Schneir, R. Sonnenfeld, and P. K. Hansma
Department of Physics, University of California, Santa Barbara, California 93106

J. Tersoff
IBM Thomas J. Watson Research Center, Yorktown Heights, New York 10598
(Received 21 April 1986)

The recent work of Park and Quate has demonstrated that atomic resolution images of graphite can be obtained in air. Here, we compare our experimental results on graphite in air and water to theoretical calculations. We present an image in close qualitative agreement with the theory and other images which can be understood by considering how images can be degraded under real experimental conditions. In addition, we present images showing graphite to be atomically flat over 10^6 Å^2 areas when imaged under water.

I. INTRODUCTION

The scanning tunneling microscope (STM) is evolving into a powerful tool for surface imaging and analysis. Milestones in this evolution have included profiling grating surfaces,[1,2] observing steps one atom high,[3–5] detailing the atomic positions in semiconductor reconstructions,[6,7] demonstrating small-scale variations in the superconducting energy gap at the surface of a thin film,[8] observing single atoms in a close-packed layer,[9–11] observing charge-density waves,[10–12] spectroscopic imagery,[13] and nanolithography.[14]

Tunneling microscopy has been used to image the surface of graphite with atomic resolution in UHV,[15] air,[16] and water[17] with similar results. These images have been in qualitative agreement with the predictions of Selloni *et al.*,[18] which are based on the general theory of Tersoff and Hamann.[19,20] One puzzling feature of some images taken with bias voltage $V \approx 0$ has been their high amplitude. Binnig *et al.* reported typical corrugation heights of 1 Å in UHV, but observed corrugation heights as large as 2.5 Å.[15] Corrugation heights of 2.5 Å were also observed in water.[17]

Recently, a simple explanation was proposed for the large corrugations on graphite. For a graphite monolayer there is a single state at E_F which determines the tunneling current in the limit of zero voltage. Within the theory of Ref. 20 the nodes in this wave function lead to singularities in the image. In reality, effects neglected in this model lead to smoothing of the singularities and a large but finite corrugation.[21]

We have obtained over five hundred atomic resolution images of graphite in air at room temperature. While the periodicity of these images is the same they differ in detail. We present an image in close agreement with theory,[21] along with representative samples of our other images, which differ from the two-dimensional theory, and explain them by considering how images can be degraded under real experimental conditions.

We have also obtained forty atomic resolution images of graphite under water. These images are similar to those obtained in air. Lower magnification images taken in water show graphite to be atomically flat over 10^6-Å^2 areas.

II. EXPERIMENTAL METHODS

The details of our bimorph STM have been described elsewhere.[11] X and Y scanning is done by moving the tip using a solid ceramic piezoelectric translator. Z motion is done by warping a piezoelectric bimorph to which the sample is attached. A drawing of our STM for work in water has also appeared elsewhere.[17] X, Y, and Z scanning is done by moving the tip using a tripod of ceramic piezoelectric tubes. The sample is immersed approximately 1 mm below the surface of the water in a 100-ml beaker or, more recently, in a 5-ml cell machined from Teflon. This microscope can, of course, also be run in air.

The sample was highly oriented pyrolytic graphite as described by Moore.[22] Fresh surfaces were exposed by cleaving the graphite using a razor blade or Scotch tape. For work with the bimorph microscope in air the sample was attached to a glass cover slide using silver paint. The cover slide was then glued to the bimorph. The tips for this microscope were made of PtIr turned on a lathe. It was prepared for atomic resolution work by increasing the gain of the feedback loop until the tip was oscillating into the surface, slowly increasing the voltage between tip and surface to 3 V, slowly decreasing the voltage between tip and surface to 10 mV, and decreasing the gain of the feedback loop until it became stable. The microscope designed for operation in water had a flat stainless-steel mount to which the sample was attached with epoxy and the tip was an etched, glass-insulated, PtIr microelectrode.[23] These microelectrodes usually give atomic resolution images with no treatment other than careful handling. Thus we now prefer them and no longer use the turned tips discussed above.

For a comparison with the graphite images we also imaged a gold film. Gold depositions took place in a diffusion-pumped chamber at 5×10^{-6} torr. The cleaned glass substrate (a number 2 cover slide) was exposed for 30 sec to glow discharge and then coated with a 7-Å chromium underlayer to improve adhesion of the gold film. The gold was evaporated from resistively heated sources and deposited at a rate of 3 Å per second to a thickness of 1000 Å, as measured by a quartz-crystal thickness monitor.

The X and Y axes of our bimorph microscope were calibrated by using the atomic lattice of another material as a reference. An identical piezoelectric translator was used to image $2H$-$TaSe_2$ under liquid-nitrogen (LN_2) by Coleman *et al.*[10] The lattice spacing of $2H$-$TaSe_2$ is known to be 3.43 Å, thus providing an accurate calibration for the translator at LN_2 temperature. Professor S. Viera kindly measured the piezoelectric constant of our translator material (C5400 from Channel Industries) at several temperatures. In particular, he found a ratio of 1.24 ± 0.04 between room-temperature and LN_2 calibrations. Using this value and the LN_2 calibration, we obtained a room-temperature calibration of 4.32 ± 0.15 Å/V which, in turn, gives 2.49 ± 0.1 Å for the lattice periodicity of graphite, in agreement with the known periodicity of 2.46 Å.

Two methods were used to calibrate the bimorph which controls the Z axis movement in our air STM.

(i) Displacement of 6 Å were measured using a commercially available magnetic phonograph cartridge (Precep A Model PC220XE).

(ii) Displacements of 5000 Å were measured using a Michelson interferometer.

Both methods yielded about 55 Å/V. The motion of the graphite mounted on the bimorph, however, was measured using the phonograph cartridge to be about 25 Å/V. The discrepancy of roughly a factor of 2 turned out to be due to the way the sample was mounted. When the sample was glued to the bimorph the entire underside of the sample was not bonded to the bimorph; typically only the corners were attached. Thus, when the bimorph warped, the distance the sample moved would not be the same as the distance the center of the bimorph moved. Given this uncertainty, our best estimate of the largest corrugation heights in the images taken with the air microscope is 2–5 Å.

The dual tripod microscope's X and Y axes were calibrated by assuming that the lattice constant of the graphite images was 2.46 Å. This was consistent with (roughly 30% less than) an upper limit we obtained from a calculation that assumed complete polarization of the piezoelectric elements and no load imposed by the tubes of the STM at right angles to the direction of motion. The Z-axis calibration was assumed to be the same as the X and Y axes because of the symmetry of the microscope design.[17] With this calibration, we found corrugation heights up to 2.5 Å in the images taken with the water microscope.

III. RESULTS AND DISCUSSION

Figure 1(a) is the calculated image for a monolayer of graphite. This image is qualitatively similar to that of

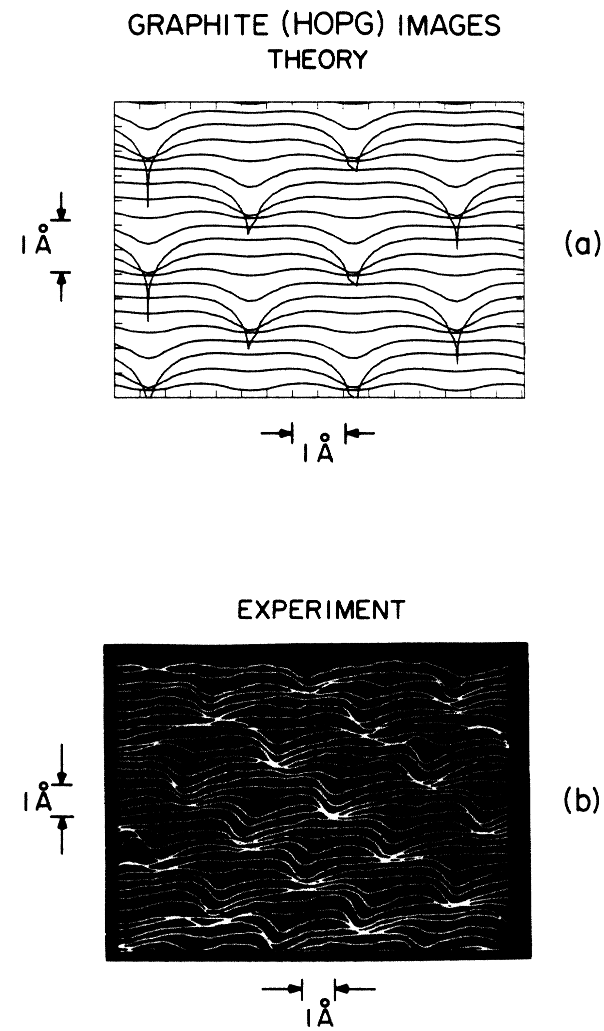

FIG. 1. (a) The calculated image for a monolayer of graphite using a recently developed theory which describes STM images of nearly-two-dimensional materials. Within the s-wave approximation the image has singularities at the sixfold hollow sites. The tic marks are at 1 a.u. (b) An experimental image of the surface of graphite in agreement with the two-dimensional theory. X and Y scales are the same. The tunneling current was 8 nA, and the tip was at $+2$ mV with respect to the graphite.

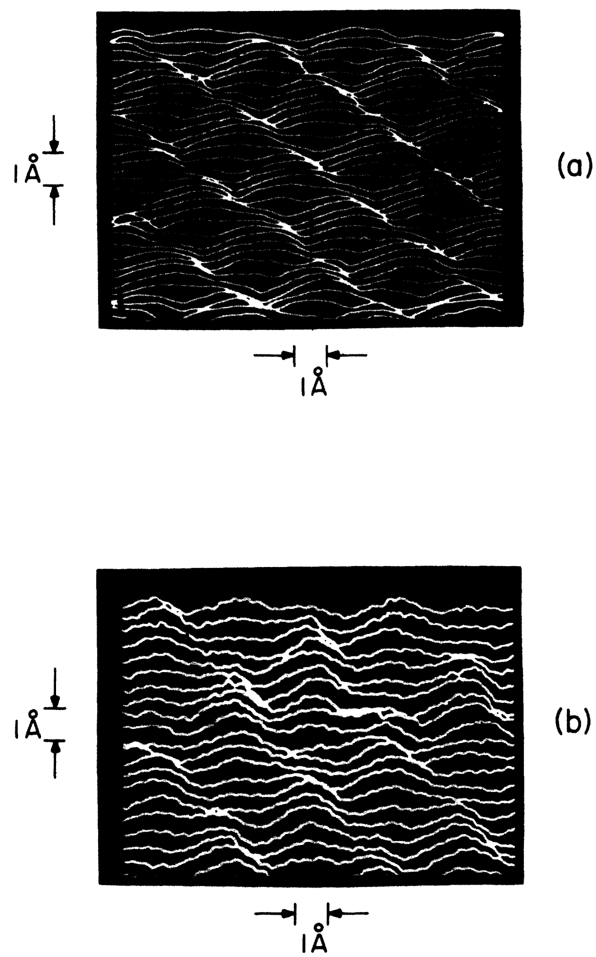

FIG. 2. (a) An image of the surface of graphite taken about 1 h before Fig. 1(b). The X and Y scales are the same. The tunneling current was 8 nA and the graphite was at $+2$ mV with respect to the graphite. (b) An image of the surface of graphite taken with tunneling current of 6 nA. The X and Y scales are the same. The graphite was at $+4$ mV with respect to the graphite.

Selloni *et al.*, but shows more extreme behavior since it represents a single monolayer in a strict zero-voltage limit.[21] Within the s-wave tip approximation the image has singularities at the sixfold hollow sites. (The singularities are not clearly resolved with the plotting grid used, i.e., most of them are asymmetrically chopped off.) The tic marks are at 1 a.u. A special feature of this surface is that the image, within the present approximations, is essentially independent of tip-surface separation, so there is only one theoretical image instead of a whole family, as in most cases.

Figure 1(b) shows an experimental image of a graphite surface taken in air. It is a photograph of a storage oscilloscope screen. The lines are Z versus X plots separated by $\Delta y = 0.25$ Å. Scanning was done left to right and top to bottom. Both theoretical and experimental images show flat plateaus with sharp dips at the sixfold hollow sites. The dips appear more rounded in the experimental image. However, if the calculated image is scaled to the experimental value of $d_{1/2}$, the distance the tip must move to change the tunneling current by a factor of $\frac{1}{2}$, agreement is good. More precisely, the theory of Ref. 21 predicts that the corrugation for graphite will scale with $d_{1/2}$. This is radically different from the usual behavior[20] where the corrugation decreases with increasing $d_{1/2}$.

Figure 2 shows two experimental images of the graphite surface taken in air, which consist of a rounded sinusoidal pattern rather than plateaus with dips as in Fig. 1. This may be due to lower resolution, which would tend to broaden the valleys and round off the plateaus. Figure 2(a) was taken about 1 h before Fig. 1(b) with the same scan speed, tunneling current, tip, and location on the graphite. This suggests that some change in the tip on the atomic scale occurred between Figs. 2(a) and 1(b) which caused the more rounded shape of Fig. 2(a). Inspection of Fig. 2(a) upside down, however, reveals that it still looks more like dips than peaks.

Although graphite surfaces should exhibit approximate threefold symmetry, all of the images obtained had varying degrees of asymmetry. Figures 3(a) and 3(b) are

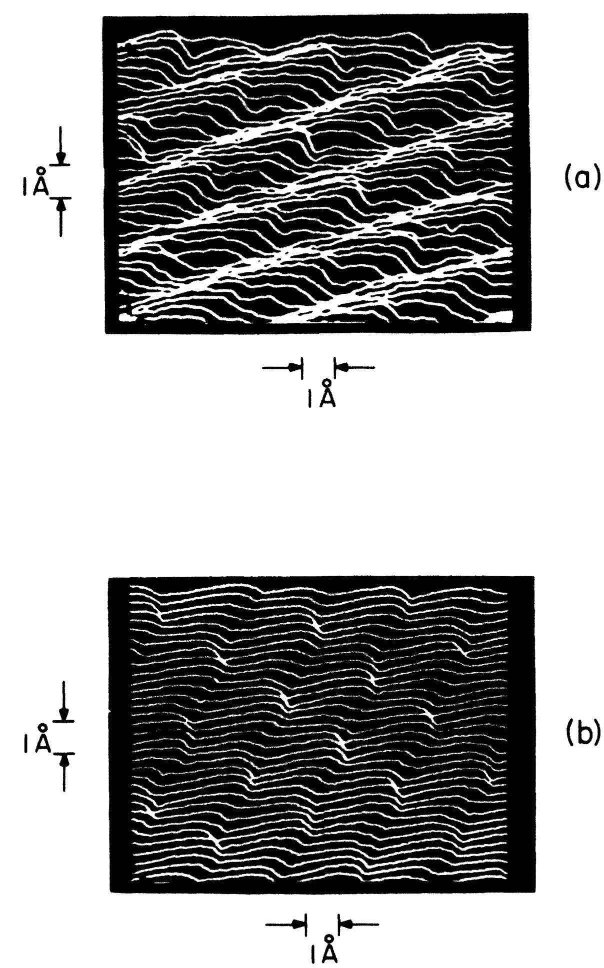

FIG. 3. (a) An asymmetric image of the surface of graphite taken with tunneling current of 4 nA. The X and Y scales are the same. The tip was at $+6$ mV with respect to the graphite. (b) An asymmetric image of the surface of graphite taken with tunneling current of 6 nA. The X and Y scales are the same. The tip was at $+4$ mV with respect to the graphite.

specific examples of asymmetric images. One possibility is that it may be due to a tilted sample. The large amplitude of the structure, 2.5 Å, relative to the nearest-neighbor distance, 2.46 Å, produced images with asymmetries comparable to those observed in Figs. 3(a) and 3(b) for tilts of order 5° in model calculations. This effect is well known in audio engineering where it is desired that if a record needle tracks along a groove that has a sinusoidal corrugation, the needle motion also be sinusoidal. However, the path of the needle becomes an increasingly asymmetric sine wave the further the needle is tilted from the perpendicular. The effect is extreme even for a 5° tilt when the corrugation height is comparable to the wavelength. The asymmetries produced in this way can resemble the experimental data.

We now believe, however, that the dominant cause of asymmetric images is an asymmetric tip as suggested by Binnig *et al.*[15] because we have recently been imaging in air, as well as in water, with the new etched tips.[23] The images are never as asymmetric as those we sometimes obtained with the PtIr tips that were turned on a lathe.

An exciting new method for imaging with a tunneling microscope has been developed by Bryant *et al.*[24] The scan speed is set high and the feedback loop gain low so the tip cannot follow the closely spaced atomic corrugations. The variations in the tunneling current are recorded. The lines on Fig. 4 are I versus X plots. The peak to valley variation in tunneling current in Fig. 4(a) is 0.2 nA, the average value of the tunneling current is about 2 nA, and the voltage between tip and sample is $+8$ mV. The corresponding quantities in Fig. 4(b), which is taken under water, are 10 nA, 10 nA, and -100 mV. In a more extensive study of the graphite surface using this imaging technique, Bryant *et al.* found that with an average current

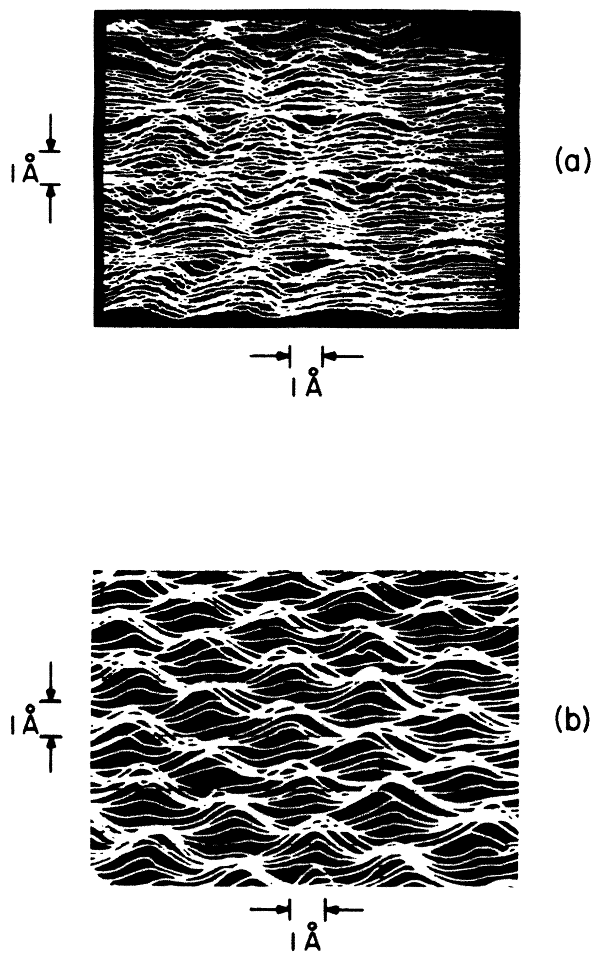

FIG. 4. (a) An image of the surface of graphite taken with the scan speed set high and the feedback loop gain low so the tip cannot follow the closely spaced atomic corrugations. The variations in tunneling current are recorded. The lines are I vs X plots offset by ΔY. The peak-to-valley variation in tunneling current is 0.2 nA, while the average value is about 2 nA. The X and Y scales are the same. (b) A similar image taken with the graphite under water. In this case the peak-to-valley variation in tunneling current is 10 nA, while the average value is 10 nA.

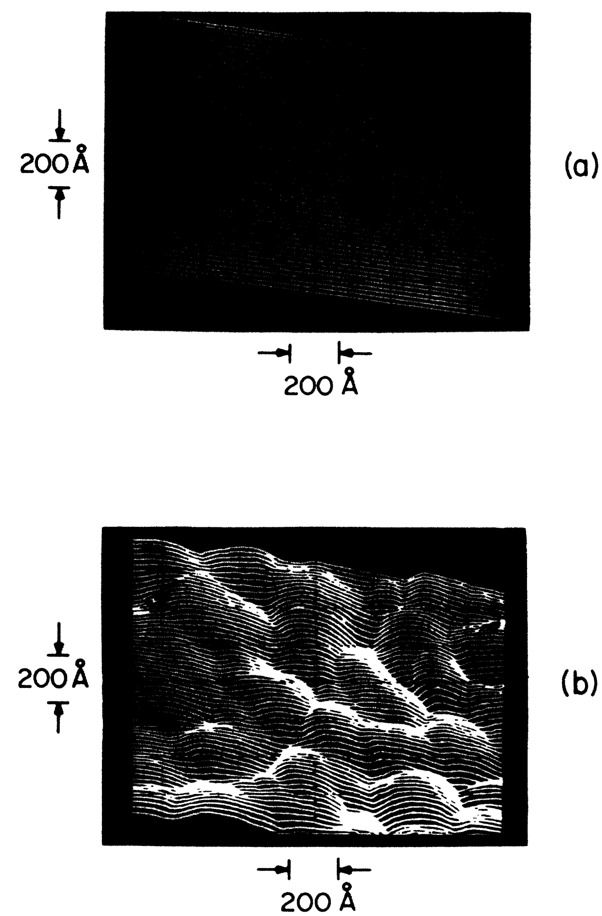

FIG. 5. (a) An image of the surface of graphite under water. The tunneling current was 10 nA and the tip was at -1 V with respect to the gold. (b) An image of the surface of a gold film taken under water. The X, Y, and Z scales are the same as in Fig. 5(a). The tunneling current was 10 nA and the tip was at -1 V with respect to the graphite. The Z sensitivity is the same as X and Y.

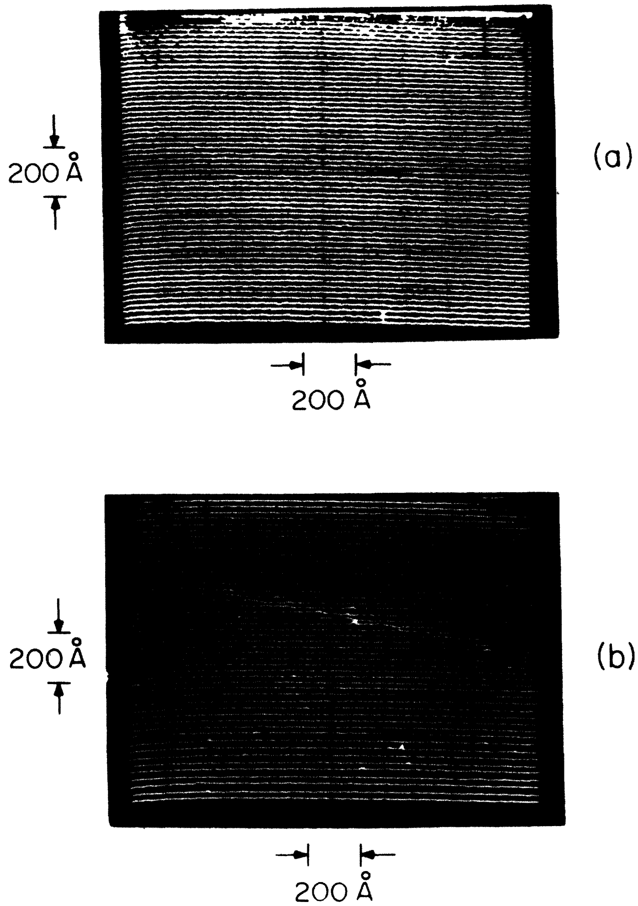

FIG. 6. Two images of the surface of graphite taken under water with the same X and Y scale. The Z sensitivity is 2.5 times greater than X and Y. The tunneling current was 5 nA and the tip was at -100 mV with respect to the graphite for both pictures.

level of 1 nA and tip-to-sample voltage of 20 mV the peak-to-valley variation in the tunneling current was 0.2 to 0.5 nA.[25] In the approximations of Ref. 21 the theory predicts zero tunneling current at the sixfold hollow sites.[21] Further work is necessary, however, to quantify the factors neglected there.

The discovery that atomic resolution tunneling microscopy may be done under water suggests the possibility of imaging biological molecules adsorbed on surfaces.[17] Graphite may be a suitable substrate for this experiment.[26] Figure 5 shows that, when imaged under water, a 1500×1500-Å area of graphite is flat compared to a gold film. The upward slope of the line scans is due to sample tilt inherent in the design of the water STM.[17] This is electronically subtracted off in Fig. 6. To better see the flatness of the surface, the Z sensitivity in Fig. 6 is 2.5 times that in Fig. 5. (The slight curvature of the braces in Fig. 6 results from nonlinearity in the subtraction electronics.)

While Fig. 6(a) was being imaged under water, atoms were visible in the tunneling current. Specifically, as the tip was being scanned at 3000 Å/sec, oscillations with a frequency near 1 kHz could be seen in an oscilloscope that was monitoring the tunneling current. These oscillations were due to passing over atoms too fast for the feedback circuit to keep the tunneling current constant. Thus the tunneling current oscillated as discussed above in connection with Fig. 4. This suggests that the entire 1500×1500-Å area was atomically flat and could be imaged with atomic resolution.

All repeatable line scans of graphite in deionized water showed the surfaces to be flat except for occasional steps such as the one shown in Fig. 6(b). These results agree with those previously obtained in air[24,26] and UHV.[15]

IV. SUMMARY

A large body of experimental data on graphite can be understood in terms of an "ideal" image consistent with theory, when combined with some simple ideas about how the features in real experimental images can be distorted.

Highly oriented pyrolytic graphite is useful as a calibration standard for the X and Y axes of tunneling microscopes. Its hexagonal, close-packed lattice of features separated by 2.46 Å gives an atomic standard that is relatively easy to image. Even when the individual features are asymmetric, the lattice retains translational symmetry. The regions of perfection extend over hundreds of angstroms.

Note added in proof. It has recently been proposed[27] that elastic deformation of the surface by the tip can produce images of the graphite surface with giant corrugations. This mechanism may contribute to some of the larger corrugation amplitudes that we have observed for low tunneling resistance.

ACKNOWLEDGMENTS

We thank S. Alexander, G. Binnig, J. Cowin, K. Dransfeld, S. C. Fain, C. Gerber, Jr., M. Dowell, and D. J. Scalapino for valuable discussions. Special thanks are due S. Viera for calibration data at various temperatures and to C. Quate for suggesting that graphite is a good calibration standard. Three of us (J. S., R. S., and P. K. H.) were supported by the National Science Foundation under Grant No. DMR-83-03623, which also provided the air table and electronics for the tunneling microscope.

[1] R. Young, Phys. Today **24(II)**, 42 (1971).
[2] R. Young, J. Ward, and F. Scire, Rev. Sci. Instrum. **47**, 1303 (1976).
[3] G. Binnig, H. Rohrer, Ch. Gerber, and E. Weibel, Phys. Rev. Lett. **49**, 57 (1982).
[4] G. Binnig and H. Rohrer, Surf. Sci. **126**, 236 (1983).
[5] G. Binnig, H. Rohrer, Ch. Gerber, and E. Stoll, Surf. Sci. **144**, 321 (1984).
[6] G. Binnig, H. Rohrer, Ch. Gerber, and E. Weibel, Phys. Rev. Lett. **50**, 120 (1983).

[7]J. A. Golovchenko, Bull. Am. Phys. Soc. **30**, 251 (1985).
[8]S. A. Elrod, A. L. de Lozanne, and C. R. Quate, Appl. Phys. Lett. **45**, 1240 (1984).
[9]C. Quate, Bull. Am. Phys. Soc. **45**, 251 (1985).
[10]R. V. Coleman, B. Drake, P. K. Hansma, and G. Slough, Phys. Rev. Lett. **55**, 4 (1985).
[11]B. Drake, R. Sonnenfeld, J. Schneir, P. K. Hansma, G. Slough, and R. V. Coleman, Rev. Sci. Instrum. **55**, 441 (1986).
[12]C. G. Slough, W. W. McNairy, R. V. Coleman, B. Drake, and P. K. Hansma, Phys. Rev. B **34**, 994 (1986).
[13]G. Binnig, Bull. Am. Phys. Soc. **30**, 251 (1985).
[14]H. Ringger, H. R. Hidber, R. Schögl, P. Oelhafen, and H.-J. Güntherodt, Appl. Phys. Lett. **46**, 832 (1985).
[15]G. Binnig, H. Fuchs, Ch. Gerber, H. Rohrer, E. Stoll, and E. Tosatti, Europhysics Lett. **1**, 31 (1986).
[16]Sang-Il Park and C. F. Quate, Appl. Phys. Lett. **48**, 112 (1986).
[17]R. Sonnenfeld and P. K. Hansma, Science **232**, 211 (1986).
[18]A. Selloni, P. Carnevali, E. Tosatti, and C. D. Chen, Phys. Rev. B **31**, 2602 (1985).
[19]J. Tersoff and D. R. Hamann, Phys. Rev. Lett. **50**, 25 (1983).
[20]J. Tersoff and D. R. Hamann, Phys. Rev. B **31**, 2 (1985).
[21]J. Tersoff, Phys. Rev. Lett. **57**, 440 (1986).
[22]A. W. Moore, in *Chemistry and Physics of Carbon*, edited by P. L. Walker, Jr. and P. A. Thrower (Dekker, New York, 1973), Vol. 11, p. 69; A. W. Moore, in *Chemistry and Physics of Carbon*, edited by P. L. Walker, Jr. and P. A. Thrower, (Dekker, New York, 1981), Vol. 17, p. 233.
[23]Part number 30-05-1 from Frederick Haer & Co. Brunswick, ME.
[24]A. Bryant, D. P. E. Smith, and C. F. Quate, Appl. Rev. Lett. **48**, 832 (1986).
[25]J. Borwick, *Sound Recording Practice* (Oxford University Press, New York, 1976), p. 296.
[26]A. M. Baro, R. Miranda, J. Alaman, N. Garcia, G. Binnig, H. Rohrer, Ch. Gerber, and J. L. Carrascosa, Nature (London) **315**, 253 (1985).
[27]J. M. Soler, A. M. Baro, N. García, and H. Rohrer, Phys. Rev. Lett. **57**, 4 (1986); H. J. Mamin, E. Ganz, D. W. Abraham, R. E. Thomson, and J. Clarke (unpublished).

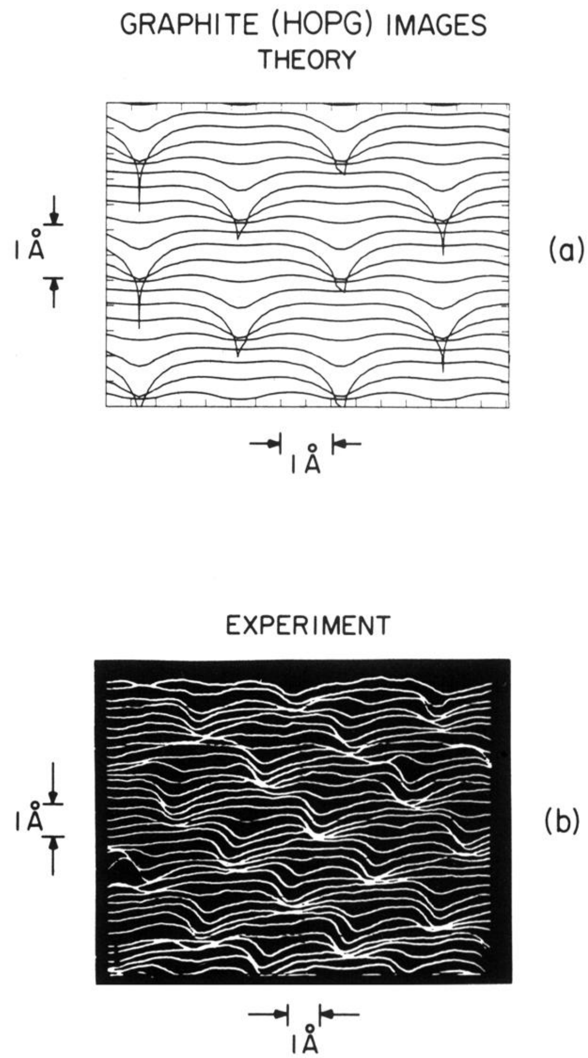

FIG. 1. (a) The calculated image for a monolayer of graphite using a recently developed theory which describes STM images of nearly-two-dimensional materials. Within the *s*-wave approximation the image has singularities at the sixfold hollow sites. The tic marks are at 1 a.u. (b) An experimental image of the surface of graphite in agreement with the two-dimensional theory. X and Y scales are the same. The tunneling current was 8 nA, and the tip was at $+2$ mV with respect to the graphite.

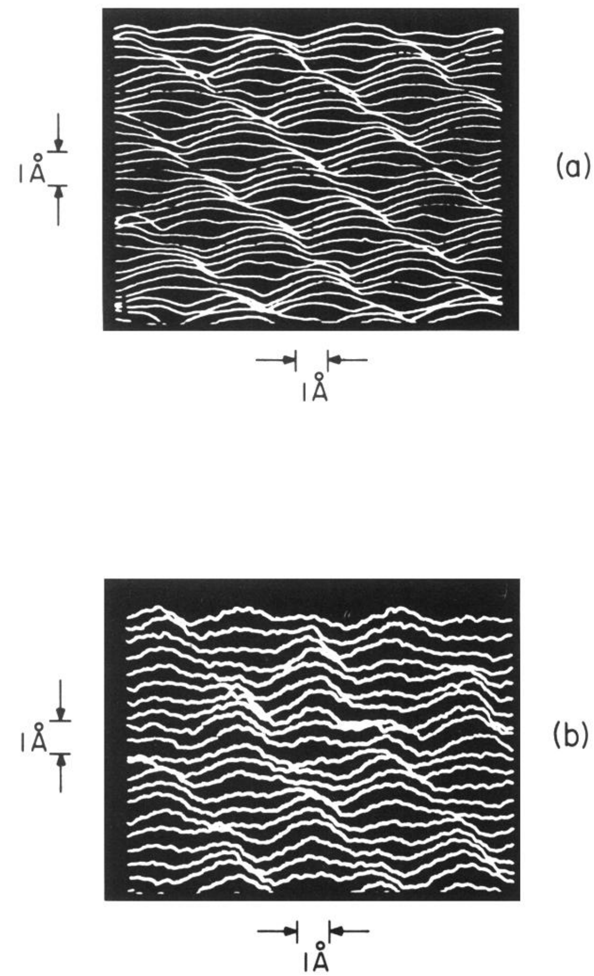

FIG. 2. (a) An image of the surface of graphite taken about 1 h before Fig. 1(b). The X and Y scales are the same. The tunneling current was 8 nA and the graphite was at $+2$ mV with respect to the graphite. (b) An image of the surface of graphite taken with tunneling current of 6 nA. The X and Y scales are the same. The graphite was at $+4$ mV with respect to the graphite.

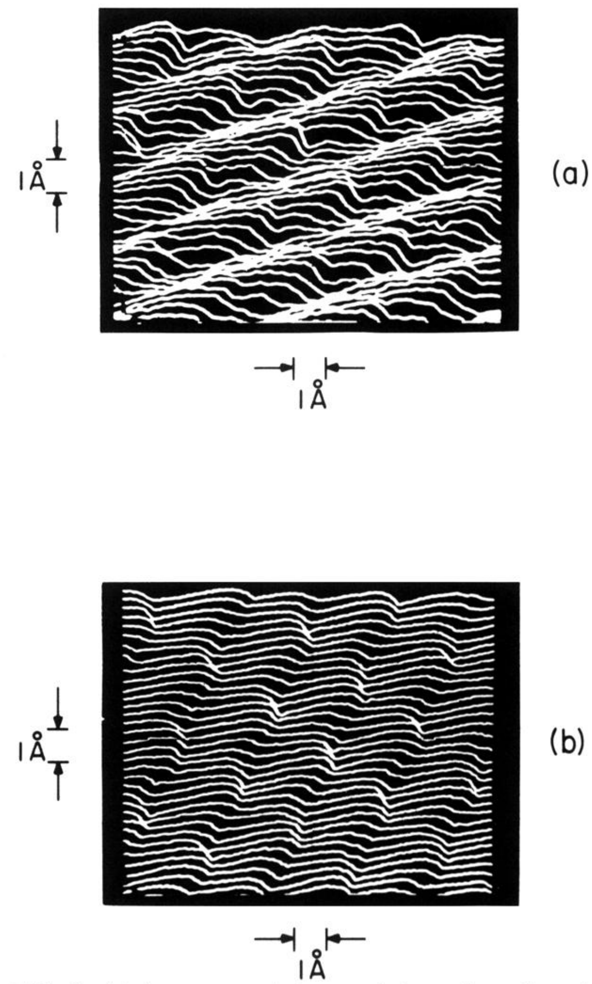

FIG. 3. (a) An asymmetric image of the surface of graphite taken with tunneling current of 4 nA. The X and Y scales are the same. The tip was at $+6$ mV with respect to the graphite. (b) An asymmetric image of the surface of graphite taken with tunneling current of 6 nA. The X and Y scales are the same. The tip was at $+4$ mV with respect to the graphite.

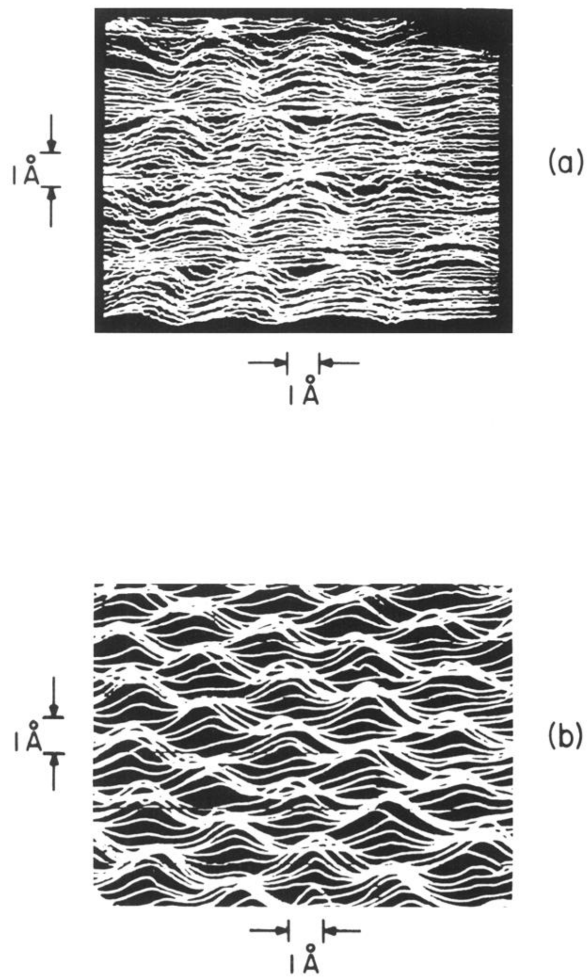

FIG. 4. (a) An image of the surface of graphite taken with the scan speed set high and the feedback loop gain low so the tip cannot follow the closely spaced atomic corrugations. The variations in tunneling current are recorded. The lines are I vs X plots offset by ΔY. The peak-to-valley variation in tunneling current is 0.2 nA, while the average value is about 2 nA. The X and Y scales are the same. (b) A similar image taken with the graphite under water. In this case the peak-to-valley variation in tunneling current is 10 nA, while the average value is 10 nA.

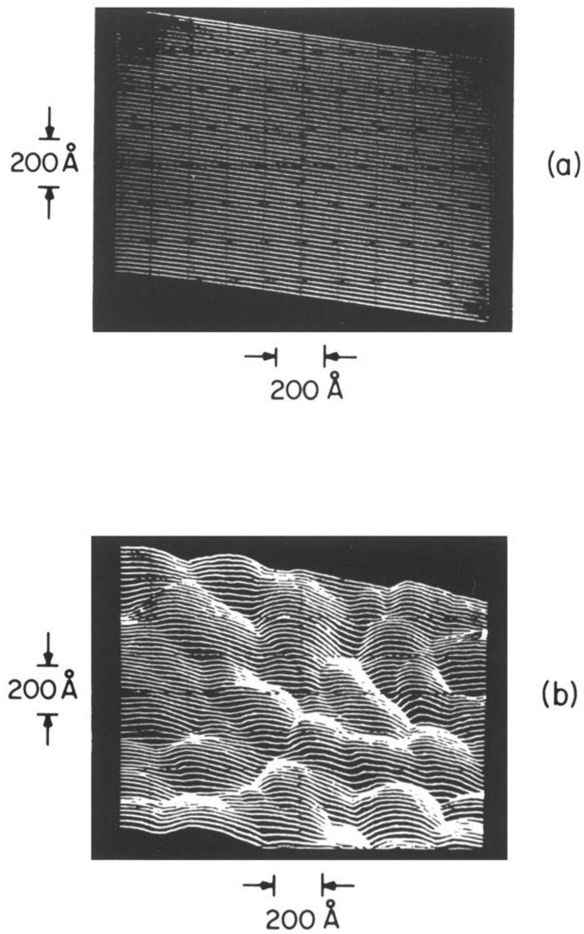

FIG. 5. (a) An image of the surface of graphite under water. The tunneling current was 10 nA and the tip was at -1 V with respect to the gold. (b) An image of the surface of a gold film taken under water. The X, Y, and Z scales are the same as in Fig. 5(a). The tunneling current was 10 nA and the tip was at -1 V with respect to the graphite. The Z sensitivity is the same as X and Y.

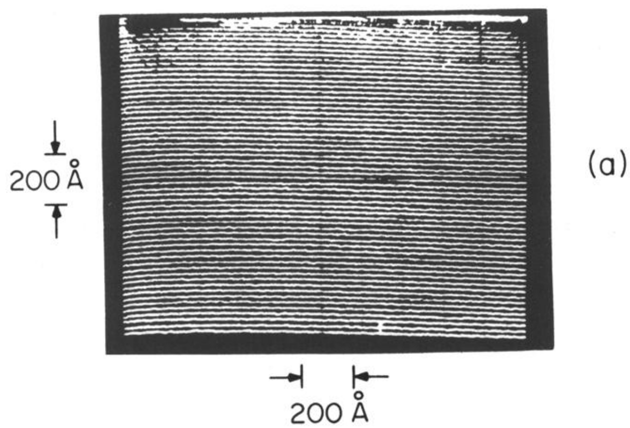

FIG. 6. Two images of the surface of graphite taken under water with the same X and Y scale. The Z sensitivity is 2.5 times greater than X and Y. The tunneling current was 5 nA and the tip was at -100 mV with respect to the graphite for both pictures.